Research Square

Preprints are preliminary reports that have not undergone peer review.
They should not be considered conclusive, used to inform clinical practice,
or referenced by the media as validated information.

Complementary Value of Hyperreflective Foci Reflectivity for Retinal Disease Beyond Count and Area

Hanji Zhang
Tianjin Medical University Eye Hospital
Yunhan Yin
Tianjin Medical University
Hongchang Wu
Zhengzhou Yangcheng hospital
Shaoyan Xia
xiashaoyan@tmu.edu.cn

Tianjin Medical University

Research Article

Keywords: optical coherence tomography, hyperreflective foci, retinal diseases, quantitative imaging

Posted Date: November 18th, 2026

DOI: https://doi.org/10.21203/rs.3.rs-10851387/v1

License: This work is licensed under a Creative Commons Attribution 4.0 International License.
Read Full License

Additional Declarations: No competing interests reported.

Abstract

Purpose: To determine whether hyperreflective foci (HRF) reflectivity on optical coherence tomography (OCT) provides complementary information beyond HRF count and total area across retinal diseases.

Methods: This retrospective study included 183 eyes from 122 patients. HRF count, total area, and mean reflectivity were quantified on OCT B-scans using ImageJ. Generalized linear mixed models were used to compare parameters across disease groups. Multinomial logistic regression and ablation analysis evaluated the contribution of mean reflectivity.

Results: HRF count and total area were highest in diabetic retinopathy (DR), followed by retinal vein occlusion (RVO) and age-related macular degeneration (AMD). Mean reflectivity also decreased significantly from AMD to DR to RVO. Removing mean reflectivity reduced the area under the curve (AUC) from 0.904 to 0.691, compared with 0.864 after removal of count and total area ($P < 0.001$). Among no apparent diabetic retinopathy (NDR), DR, and diabetic macular edema (DME), removal of count and total area reduced the AUC from 0.927 to 0.798, and removal of mean reflectivity yielded an AUC of 0.812. Count and total area contributed more strongly to distinguishing NDR from DR ($P < 0.001$), whereas mean reflectivity contributed more to comparisons involving DME ($P < 0.05$).

Conclusion:HRF reflectivity provided complementary discriminatory information beyond count and total area, particularly among AMD, DR, and RVO. In contrast, conventional HRF measures were more informative for distinguishing NDR from DR.

Introduction

Age-related macular degeneration (AMD), diabetic retinopathy (DR), and retinal vein occlusion (RVO) are among the most common retinal disorders associated with irreversible vision loss worldwide. Optical coherence tomography (OCT) has become an essential imaging modality for the clinical evaluation of these retinal disorders by providing noninvasive, high-resolution visualization of retinal microstructural changes and various imaging biomarkers, including hard exudates, subretinal fluid, and drusen. Among these biomarkers, hyperreflective foci (HRF) have attracted increasing attention because they occur in multiple retinal diseases and have been associated with disease severity, progression and visual outcomes.

HRF were initially described in diabetic macular edema (DME) and exudative AMD by Bolz et al. and Coscas et al., respectively [1, 2]. Although definitions vary among studies, HRF are generally characterized as small, discrete, punctate hyperreflective lesions within the inner or outer retinal layers, with reflectivity comparable to or greater than that of the retinal pigment epithelium (RPE) or retinal nerve fiber layer and without posterior shadowing [1–5]. Quantitative assessment of HRF has primarily focused on count and area, which characterize overall lesion burden. Reflectivity represents a distinct OCT signal property and may provide information not captured by burden measures alone.

The potential relevance of HRF reflectivity is supported by the heterogeneous pathological substrates proposed for these lesions. In AMD, HRF are thought to represent the migration of transdifferentiated RPE cells and activation of microglia [6–9]. As for DR, HRF are considered to represent extravasated lipid or lipoprotein deposits associated with blood-retinal barrier disruption, as well as activated microglia [10]. In RVO, HRF formation has been hypothesized to be associated with acute or subacute venous pressure overload and capillary nonperfusion, which may promote extravasation of blood components, lipid accumulation, and secondary microglial recruitment [11]. These differences in composition may influence OCT signal characteristics. However, structural OCT cannot directly determine the cellular or molecular composition of HRF, and the relationship between pathological substrate and reflectivity remains incompletely understood.

Previous studies have associated HRF with disease progression, treatment response, and visual outcomes in AMD, DR, DME, and RVO [10, 12–27]. However, most studies have evaluated individual diseases and emphasized conventional burden measures, particularly HRF count and area. Direct comparisons of HRF quantitative characteristics across retinal diseases remain limited, and whether reflectivity provides discriminatory information beyond HRF count and total area therefore remains unclear.

Accordingly, this study compared HRF count, total area, and mean reflectivity across AMD, DR, and RVO, and across diabetic retinal conditions including no apparent diabetic retinopathy (NDR), DR without DME, and DME. Generalized linear mixed models were used to compare individual HRF parameters across disease groups, and multinomial logistic regression with ablation analysis was used to evaluate the complementary contribution of mean reflectivity beyond count and total area.

Materials and Methods

Ethics approval

This retrospective study was conducted in accordance with the Declaration of Helsinki and was approved by the Medical Ethics Committee. The requirement for informed consent was waived because the study involved only the retrospective analysis of existing clinical records and previously acquired OCT images. No additional examinations or interventions were performed for the purposes of this study.

Study population and group definitions

Patients diagnosed with AMD, DR, or RVO were retrospectively identified between 2021 and 2024. A primary analysis was performed among eyes with AMD, DR, and RVO. In addition, a separate analysis was conducted within the diabetic cohort according to diabetic retinal status. The diabetic cohort was categorized into three mutually exclusive groups, NDR, DR without DME, and DME. The DR cohort included in the diabetic analysis was the same cohort used in the AMD, DR, and RVO comparison.

Diagnoses were independently confirmed by two ophthalmologists according to established international guidelines, and any diagnostic discrepancies were resolved by a senior specialist.

OCT image acquisition and quality criteria

OCT images of both eyes were acquired using the Cirrus HD-OCT (Carl Zeiss Meditec, Dublin, CA, USA) with a 512 × 128 macular cube protocol, covering a 6 × 6 mm area centered on the fovea. Only scans with proper centration and a signal strength score at least 7/10 were included in the quantitative analysis. All images were acquired using the same device and scan protocol.

HRF identification and quantitative image analysis

All B-scans within the macular cube scan were reviewed, and B-scans containing identifiable HRF were selected for quantitative analysis. Selected B-scans were imported into ImageJ software (version 1.54; National Institutes of Health, Bethesda, MD, USA) in accordance with previously described protocols [16, 19, 28, 29]. HRF were defined as discrete hyperreflective lesions within the inner or outer retinal layers. Lesions with a minimum area of three pixels and reflectivity equal to or greater than the predefined threshold were included. The reflectivity threshold was defined as two standard deviations above the mean RPE reflectivity measured from 20 healthy control eyes with clear vitreous and no apparent retinal abnormalities. To minimize interference from retinal structures or imaging artifacts, structures corresponding to vessel cross-sections, shadowing artifacts, and subretinal or choroidal lesions were excluded.

The Analyze Particles function in ImageJ was used to extract 13 quantitative parameters. HRF count, total area, and mean reflectivity were prespecified as primary analytical metrics. Count and total area represented overall HRF burden, whereas mean reflectivity represented the average reflectivity of individual HRF. The remaining morphological and reflectivity parameters, including circularity, perimeter, Feret-related measurements, major and minor axis lengths, angle, median, and mode, were analyzed as exploratory outcomes and are defined in Supplementary Table S1. Circularity was used to characterize shape regularity, with values approaching 1.00 indicating a more circular shape and lower values indicating greater elongation. The Feret diameter was defined as the maximum distance between two parallel tangents along the boundary of each HRF. OCT image review and HRF parameter extraction were independently performed by two trained observers blinded to patients' clinical information and disease diagnoses. Any discrepancies between observers were resolved by consensus with a third senior ophthalmologist.

Statistical analysis

All statistical analyses were performed using R software version 4.5.2 (R Foundation for Statistical Computing, Vienna, Austria). Because multiple OCT B-scans could be obtained from the same eye and

both eyes could be included from the same patient, the observations had a hierarchical structure, with B-scans nested within eyes and eyes nested within patients. The analytical workflow was executed in two sequential phases. First, to explore whether individual HRF parameters differed significantly across disease groups while accounting for the correlation of repeated observations, generalized linear mixed models were constructed with each HRF parameter as the dependent variable, disease group as the fixed effect, and random intercepts for patient and eye nested within patient. Age was included as a covariate because significant differences in age were observed among disease cohorts. HRF count was modeled using a negative binomial distribution, whereas continuous parameters were analyzed using appropriate distributions and link functions according to their distributional characteristics. Post hoc pairwise comparisons were performed when significant group differences were identified. P values from multiple HRF parameter comparisons were adjusted using the Benjamini–Hochberg procedure. An adjusted P value < 0.05 was considered statistically significant.

Second, multinomial logistic regression models were constructed to evaluate whether mean reflectivity provided complementary discriminatory value beyond conventional HRF burden metrics. A full model incorporating HRF count, total area, and mean reflectivity was established. Two ablation models were subsequently generated by respectively removing burden and reflectivity from the full model. Model performance was evaluated using macro-averaged area under the curve (AUC). The impact of individual feature categories was assessed by comparing AUC reduction between the full model and each ablation model. DeLong's test was used to compare correlated receiver operating characteristic (ROC) curves and determine whether removal of mean reflectivity or conventional HRF burden metrics significantly affected model discrimination.

Results

Demographic and Clinical Baseline Characteristics

A total of 183 eyes from 122 patients were included, comprising 15 patients with AMD, 23 with RVO, 18 with NDR, 47 with DR without DME, and 19 with DME. The mean age was 61.3 ± 12.9 years, and 72 patients (59.0%) were men. Age differed among the clinical groups (P = 0.044), whereas sex distribution did not (P = 0.139).

Difference in HRF count, total area, and Mean Reflectivity Across AMD, DR, and RVO

The HRF count was 3.51 ± 1.60 in AMD, 5.26 ± 2.46 in RVO, and 6.95 ± 3.57 in DR. GLMM analysis revealed a significant difference among the three cohorts (P < 0.001). Post-hoc pairwise comparisons demonstrated that eyes with DR had a significantly higher HRF count than those with AMD (P < 0.0001) and RVO (P = 0.005, Fig. 1a). Additionally, the HRF count in RVO eyes was significantly higher than in AMD eyes (P = 0.004). A similar pattern was observed for the total HRF area (P < 0.001). Post-hoc

pairwise analyses revealed that the total HRF area in DR eyes was significantly larger than in AMD eyes ($P < 0.0001$) and RVO eyes ($P = 0.014$, Fig. 1b). Furthermore, RVO eyes exhibited a significantly greater total HRF area compared with AMD eyes ($P = 0.017$). Beyond count and area, the comparison of mean reflectivity between disease cohorts revealed statistically significant differences across all pairwise tests (all $P < 0.0001$, Fig. 1c). Results of the exploratory analyses of additional features are provided in Supplementary Table S2.

Figure 1 HRF count, total area, and mean reflectivity across AMD, DR, and RVO

Differences in HRF Count, Total Area, and Mean Reflectivity Across NDR, DR, and DME

In the diabetic retinal condition analysis, HRF parameters demonstrated distinct patterns among NDR, DR without DME, and DME. HRF count showed a graded increase across the three groups, with values of 1.79 ± 0.63 in NDR, 6.95 ± 3.57 in DR without DME, and 8.77 ± 2.74 in DME. All pairwise comparisons were statistically significant (overall $P < 0.001$, all pairwise $P < 0.05$; Fig. 2a). Similarly, total HRF area increased progressively across the three groups, rising from NDR to DR and peaking in DME (overall $P < 0.001$; Fig. 2b). In contrast to HRF burden, mean reflectivity showed a different distribution pattern. DME showed significantly higher mean reflectivity than both NDR ($P = 0.004$) and DR ($P < 0.001$; Fig. 2c), whereas no significant difference was observed between NDR and DR. Exploratory comparisons of the remaining HRF features are presented in Supplementary Table S2.

Figure 2 HRF count, total area, and mean reflectivity among NDR, DR without DME, and DME

Complementary Discriminatory Value and Ablation Analysis

The combined logistic regression models, including HRF burden and reflectivity parameters, achieved an overall AUC of 0.904 (95% CI, 0.891–0.917), with an overall accuracy of 81.62%, sensitivity of 86.05% and specificity of 81.77% across AMD, DR, and RVO. Specifically, in pairwise discrimination, the model effectively separated AMD from DR (AUC = 0.904), AMD from RVO (AUC = 0.975), and DR from RVO (AUC = 0.833). Meanwhile, the combined logistic regression models achieved an overall AUC of 0.927 (95% CI, 0.916–0.937), with an overall accuracy of 82.43%, sensitivity of 90.13% and specificity of 86.20% across NDR, DR and DME. In pairwise discrimination, the model effectively separated NDR from DR (AUC = 0.948), NDR from DME (AUC = 0.934), and DR from DME (AUC = 0.898).

To explore the incremental discriminatory contribution of conventional quantitative metrics versus reflectivity, two ablation studies were conducted. Two individual regression models were developed by respectively excluding burden parameters and mean reflectivity. Across the AMD, DR, and RVO cohorts, ablating HRF burden parameters reduced classification performance to an AUC of 0.864 (95% CI, 0.849–0.879), whereas removing mean reflectivity resulted in a lower AUC of 0.691 (95% CI, 0.658–0.723). DeLong's test revealed significant overall differences across the models ($P < 0.001$). In pairwise

comparisons between the two ablated models, removing mean reflectivity led to a significantly greater performance drop (P < 0.001). However, in the AMD versus RVO comparison, ablating conventional burden metrics caused no significant loss compared with the full model (P = 0.277). Detailed results are presented in Fig. 3 and Table 1.

Furthermore, across the NDR, DR, and DME cohorts, removal of conventional burden metrics (count and area) resulted in an AUC of 0.798 (95% CI, 0.779–0.815), whereas exclusion of mean reflectivity yielded an AUC of 0.812 (95% CI, 0.792–0.829). Specifically, in the NDR versus DR comparison, removal of count and area led to a significantly greater decline in AUC than exclusion of mean reflectivity, whereas excluding mean reflectivity alone did not significantly reduce model performance compared with the full model (P = 0.100). In contrast, for the other disease comparisons, DeLong's test demonstrated that exclusion of mean reflectivity resulted in a significantly greater AUC reduction than removal of conventional HRF parameters (P < 0.05). Detailed results are presented in Fig. 4 and Table 1.

Discussion

This study evaluated whether mean HRF reflectivity provided complementary discriminatory information beyond conventional HRF burden measures. The principal finding was that mean reflectivity contributed complementary information to the discrimination among AMD, DR, and RVO. However, the incremental value of reflectivity was not uniform across all comparisons. Reflectivity contributed limited information for distinguishing NDR from DR but contributed more strongly to comparisons involving DME.

Table 1
Incremental discriminatory value of HRF burden and mean reflectivity based on ablation analysis.

AMD vs. DR	Full model	Model 1	Model 2	$P_{\text{Full vs Model 1}}$	$P_{\text{Full vs Model 2}}$	$P_{\text{Model 1 vs Model 2}}$
	0.904	**0.666**	**0.821**	**< 0.001**	**< 0.001**	**< 0.001**
AMD vs. RVO	0.975	0.729	0.971	< 0.001	0.277	< 0.001
DR vs. RVO	0.833	0.675	0.800	< 0.001	< 0.001	< 0.001
NDR vs. DR	0.948	0.936	0.689	0.256	< 0.001	< 0.001
NDR vs. DME	0.934	0.751	0.833	< 0.001	< 0.001	0.01
DR vs. DME	0.898	0.749	0.873	< 0.001	< 0.001	< 0.001

AMD, age-related macular degeneration; DR, diabetic retinopathy; RVO, retinal vein occlusion; NDR, no apparent diabetic retinopathy; DME, diabetic macular edema; HRF, hyperreflective foci; AUC, area under the receiver operating characteristic curve. The full model included HRF count, total area, and mean

reflectivity. Model 1 excluded mean reflectivity, whereas Model 2 excluded HRF count and total area. Values are AUCs. P values were calculated using DeLong's test.

The findings closely corroborate previous studies showing that HRF count and total area differ significantly among retinal diseases. Across AMD, DR, and RVO, both HRF count and total area demonstrated significant intergroup differences, with greatest observed in DR, followed by RVO and AMD. This pattern is highly consistent with previous comparative studies reporting greater HRF accumulation in DR than in AMD or RVO [19, 21]. A similar pattern was observed within the diabetic groups. HRF count and total area increased progressively from NDR to DR and then to DME, in agreement with previous reports associating increased HRF burden with the severity[30].

Beyond confirming these established patterns, this study additionally observed that reflectivity decreased from AMD to DR and RVO, whereas it was comparable between NDR and DR but significantly higher in DME. Interestingly, one study reported higher normalized HRF reflectivity in AMD than in DR [19], whereas another reported higher HRF reflectivity in DR than in RVO [21]. Within diabetic retinal conditions, a previous OCT angiography study found no significant difference in HRF decorrelation signal between non-proliferative and PDR but identified a difference between DR and DME [30]. These studies collectively suggest that HRF signal characteristics may vary across retinal diseases and diabetic retinal conditions. However, previous studies evaluated individual disease comparisons and did not determine whether reflectivity provided discriminatory information beyond conventional HRF burden measures. By assessing multiple disease groups within a common quantitative framework and comparing full and ablation models, the present study extends previous evidence by directly evaluating the incremental contribution of reflectivity beyond count and total area.

The ablation analysis translated these parameter differences into model evidence. Among AMD, DR, and RVO, removal of mean reflectivity reduced the overall AUC from 0.904 to 0.691, whereas removal of count and total area reduced the AUC to 0.864. The larger performance reduction after removal of reflectivity indicates that its contribution to disease discrimination was not fully represented by conventional burden measures. In the diabetic cohort, removal of count and total area and removal of mean reflectivity reduced the overall AUC from 0.927 to 0.798 and 0.812, respectively. However, the relative contributions of burden and reflectivity differed across pairwise comparisons. Conventional measures contributed more strongly to discrimination between NDR and DR without DME, whereas reflectivity contributed more strongly to comparisons involving DME. Reflectivity should therefore be considered an additional quantitative OCT feature rather than a replacement for established conventional HRF measures. Moreover, because OCT signal intensity is affected by device characteristics, acquisition quality, image export, and normalization procedures, standardization of image acquisition, reference selection, and reflectivity calculation will be necessary before measurements can be compared across devices, institutions, or study populations.

A potential biological basis for the incremental information provided by reflectivity is the pathological heterogeneity of HRF. Count and total area quantify the number and overall extent of HRF but do not

characterize variation in OCT signal intensity, which may be associated with differences in lesion composition. Although HRF share similar appearances on OCT, histological and experimental studies have associated them with activated microglia [10, 31], migrating or transdifferentiated RPE cells [6–9], extravasated lipid or proteinaceous material [10, 32, 33], and other inflammatory or vascular components [11]. HRF may therefore represent a family of morphologically similar but biologically heterogeneous OCT findings rather than a single pathological entity. This interpretation is consistent with previous studies proposing multiple pathological origins of HRF [3, 5, 34]. Frizziero et al. further categorized HRF into inflammatory, pigmentary, vascular, and exudative subtypes based primarily on morphological and reflectivity characteristics [3]. These proposed pathological differences provide a plausible basis for variation in HRF signal characteristics.

Against this background of pathological heterogeneity, the reflectivity pattern may partly reflect differences in the predominant substrates of HRF. The higher mean reflectivity observed in AMD may be related to pigmented RPE-derived cells or melanophages, whose melanosomes and melanolipofuscin can produce strong OCT backscattering [2, 6, 31, 35]. In DR, HRF may represent a heterogeneous mixture of inflammatory cells and extravasated lipid or proteinaceous material, potentially accounting for their intermediate reflectivity [33, 36]. In RVO, HRF have been associated with the accumulation of extravasated blood constituents within edematous retinal tissue and with vascular and exudative processes [11, 27]. These compositional differences could contribute to the lower mean reflectivity observed in RVO. However, direct histological evidence linking HRF composition to OCT reflectivity, particularly in RVO, remains limited. Therefore, these explanations should be considered hypotheses.

The value of reflectivity within the diabetic cohort may reflect a different stage of HRF compositional change. Reflectivity added limited discriminatory information between NDR and DR, suggesting that differences between these groups were expressed primarily through an increase in HRF burden rather than through marked changes in HRF composition. By contrast, reflectivity contributed more strongly to comparisons involving DME. Increased vascular permeability and blood-retinal barrier disruption in DME may promote the accumulation of lipid and proteinaceous material, thereby altering HRF reflectivity characteristics in ways not captured by count and total area alone [10, 36–38]. Thus, reflectivity may become more informative when macular edema is accompanied by changes in the exudative composition of HRF. However, this interpretation remains inferential and requires confirmation using histological or multimodal imaging reference standards.

Several limitations should be acknowledged. First, the retrospective design and relatively limited sample size may introduce potential selection bias and restrict the generalizability of the findings. Second, HRF identification and feature extraction were semiautomated and therefore remained dependent on observer input. Although images were reviewed by trained observers, the reproducibility of the complete measurement workflow should be evaluated in independent datasets. Third, OCT signal intensity is influenced by device characteristics, acquisition quality, image export, and normalization procedures. Because reflectivity was measured using a single device and image-analysis workflow, the values should not be assumed to be directly transferable across OCT systems or institutions. Fourth, the pathological

interpretation of HRF reflectivity was inferential because no histological or multimodal imaging reference standard was available. External validation using standardized OCT acquisition and reflectivity measurements is required before clinical application.

In conclusion, mean HRF reflectivity provided complementary information beyond conventional measures, although its incremental value varied across disease comparisons. Reflectivity contributed strongly to discrimination among AMD, DR, and RVO and to comparisons involving DME but added limited information for distinguishing NDR from DR. These findings support further evaluation of HRF reflectivity as an additional quantitative OCT feature beyond count and total area. Validation in larger prospective cohorts using standardized OCT acquisition and automated reflectivity measurements is required before clinical application.

Declarations

Funding

This study was supported by Tianjin Municipal Education Commission Research Project (grant number 2024KJ227).

Competing Interests

The authors have no relevant financial or non-financial interests to disclose.

Author Contributions

Hanji Zhang and Shaoyan Xia contributed to the study conception, design, and methodology. Hanji Zhang, Yunhan Yin, and Hongchang Wu performed data curation and investigation. Hanji Zhang conducted the formal analysis and prepared the visualizations. Yunhan Yinperformed data validation.Hanji Zhang wrote the original draft of the manuscript. Shaoyan Xia acquired funding, administered and supervised the project, and reviewed and edited the manuscript. All authors reviewed and approved the final manuscript.

Ethics Approval

This study was performed in accordance with the Declaration of Helsinki. Approval was granted by the Ethics Committee of Zhengzhou Yangcheng Hospital.

Consent to Participate

The requirement for informed consent was waived by the Ethics Committee because of the retrospective nature of the study.

Consent to Publish

Not Applicable

Data Availability

The datasets are not publicly available due to patient privacy considerations but are available from the corresponding author on reasonable request and subject to applicable ethical approval.

References

1. Bolz M, Schmidt-Erfurth U, Deak G, Mylonas G, Kriechbaum K, Scholda C, et al (2009)Optical coherence tomographic hyperreflective foci: a morphologic sign of lipid extravasation in diabetic macular edema.Ophthalmology 116:914–920. https://doi.org/10.1016/j.ophtha.2008.12.039
2. Coscas G, De Benedetto U, Coscas F, Li Calzi CI, Vismara S, Roudot-Thoraval F, et al (2013)Hyperreflective dots: a new spectral-domain optical coherence tomography entity for follow-up and prognosis in exudative age-related macular degeneration.Ophthalmologica 229:32–37. https://doi.org/10.1159/000342159
3. Frizziero L, Midena G, Danieli L, Torresin T, Perfetto A, Parrozzani R, et al (2025)Hyperreflective Retinal Foci (HRF): Definition and Role of an Invaluable OCT Sign.J Clin Med 14:https://doi.org/10.3390/jcm14093021
4. Fragiotta S, Abdolrahimzadeh S, Dolz-Marco R, Sakurada Y, Gal-Or O, Scuderi G (2021)Significance of Hyperreflective Foci as an Optical Coherence Tomography Biomarker in Retinal Diseases: Characterization and Clinical Implications.J Ophthalmol 2021:6096017. https://doi.org/10.1155/2021/6096017
5. Boscia G, Feo A, Quarta A, Stradiotto E, Forte P, Termite AC, et al (2026)Intraretinal hyperreflective foci: Pathophysiology, imaging features, and clinical implications across retinal diseases.Prog Retin Eye Res 112:101464. https://doi.org/10.1016/j.preteyeres.2026.101464
6. Balaratnasingam C, Messinger JD, Sloan KR, Yannuzzi LA, Freund KB, Curcio CA (2017)Histologic and Optical Coherence Tomographic Correlates in Drusenoid Pigment Epithelium Detachment in Age-Related Macular Degeneration.Ophthalmology 124:644–656. https://doi.org/10.1016/j.ophtha.2016.12.034
7. Bousquet E, Abraham N, Estawro R, Khadka S, Voichanski S, Mafi M, et al (2024)SUB RETINAL PIGMENT EPITHELIUM HYPOREFLECTIVE SPACES PRECEDING LARGE DRUSEN COLLAPSE.Retina 44:2041–2048. https://doi.org/10.1097/iae.0000000000004233

8. Cao D, Leong B, Messinger JD, Kar D, Ach T, Yannuzzi LA, et al (2021)Hyperreflective Foci, Optical Coherence Tomography Progression Indicators in Age-Related Macular Degeneration, Include Transdifferentiated Retinal Pigment Epithelium.Invest Ophthalmol Vis Sci 62:34. https://doi.org/10.1167/iovs.62.10.34
9. Curcio CA, Zanzottera EC, Ach T, Balaratnasingam C, Freund KB (2017)Activated Retinal Pigment Epithelium, an Optical Coherence Tomography Biomarker for Progression in Age-Related Macular Degeneration.Invest Ophthalmol Vis Sci 58:Bio211-bio226. https://doi.org/10.1167/iovs.17-21872
10. Vujosevic S, Bini S, Midena G, Berton M, Pilotto E, Midena E (2013)Hyperreflective intraretinal spots in diabetics without and with nonproliferative diabetic retinopathy: an in vivo study using spectral domain OCT.J Diabetes Res 2013:491835. https://doi.org/10.1155/2013/491835
11. Ogino K, Murakami T, Tsujikawa A, Miyamoto K, Sakamoto A, Ota M, et al (2012)Characteristics of optical coherence tomographic hyperreflective foci in retinal vein occlusion.Retina 32:77–85. https://doi.org/10.1097/IAE.0b013e318217ffc7
12. Berni A, Shen M, Cheng Y, Herrera G, Hiya F, Liu J, et al (2024)The Total Macular Burden of Hyperreflective Foci and the Onset of Persistent Choroidal Hypertransmission Defects in Intermediate AMD.Am J Ophthalmol 267:61–75. https://doi.org/10.1016/j.ajo.2024.06.023
13. Berni A, Kastner JD, Shen M, Cheng Y, Herrera G, Hiya F, et al (2025)Hyperreflective Foci Along the Retinal Pigment Epithelium Predict the Onset of Large Choroidal Hypertransmission Defects in Age-Related Macular Degeneration.Am J Ophthalmol 274:76–90. https://doi.org/10.1016/j.ajo.2025.02.021
14. Fragiotta S, Rossi T, Cutini A, Grenga PL, Vingolo EM (2018)PREDICTIVE FACTORS FOR DEVELOPMENT OF NEOVASCULAR AGE-RELATED MACULAR DEGENERATION: A Spectral-Domain Optical Coherence Tomography Study.Retina 38:245–252. https://doi.org/10.1097/iae.0000000000001540
15. Flores R, Carneiro Â, Tenreiro S, Seabra MC (2021)Retinal Progression Biomarkers of Early and Intermediate Age-Related Macular Degeneration.Life (Basel) 12:https://doi.org/10.3390/life12010036
16. Nassisi M, Fan W, Shi Y, Lei J, Borrelli E, Ip M, et al (2018)Quantity of Intraretinal Hyperreflective Foci in Patients With Intermediate Age-Related Macular Degeneration Correlates With 1-Year Progression.Invest Ophthalmol Vis Sci 59:3431–3439. https://doi.org/10.1167/iovs.18-24143
17. Borrelli E, Reibaldi M, Barresi C, Berni A, Introini U, Bandello F (2023)Choroidal Hyper-Reflective Foci in Geographic Atrophy.Invest Ophthalmol Vis Sci 64:5. https://doi.org/10.1167/iovs.64.14.5
18. Wan Z, Wu Y, Shen T, Hu C, Lin R, Ren C, et al (2024)Evaluation of inflammatory hyperreflective foci and plasma EPA as diagnostic and predictive markers for age-related macular degeneration.Front Neurosci 18:1401101. https://doi.org/10.3389/fnins.2024.1401101
19. Ashrafkhorasani M, Habibi A, Nittala MG, Yaseri M, Emamverdi M, Velaga SB, et al (2025)Spectral-domain OCT characteristics of intraretinal hyper-reflective foci associated with age-related macular

degeneration and diabetic retinopathy.Can J Ophthalmol 60:91–99. https://doi.org/10.1016/j.jcjo.2024.07.017

20. Xiaodong L, Xuejun X, Xiaojuan S, Yu H, Mingchao X (2023)Characterization of peripheral blood inflammatory indicators and OCT imaging biological markers in diabetic retinopathy with or without nephropathy.Front Endocrinol (Lausanne) 14:1160615. https://doi.org/10.3389/fendo.2023.1160615
21. Tao Y, Ge L, Su N, Li M, Fan W, Jiang L, et al (2024)Exploration on OCT biomarker candidate related to macular edema caused by diabetic retinopathy and retinal vein occlusion in SD-OCT images.Sci Rep 14:14317. https://doi.org/10.1038/s41598-024-63144-2
22. Niu S, Yu C, Chen Q, Yuan S, Lin J, Fan W, et al (2017)Multimodality analysis of Hyper-reflective Foci and Hard Exudates in Patients with Diabetic Retinopathy.Sci Rep 7:1568. https://doi.org/10.1038/s41598-017-01733-0
23. Tripathi A, Kumar P, Tulsani A, Chakrapani PK, Maiya G, Bhandary SV, et al (2023)Fuzzy Logic-Based System for Identifying the Severity of Diabetic Macular Edema from OCT B-Scan Images Using DRIL, HRF, and Cystoids.Diagnostics (Basel) 13:https://doi.org/10.3390/diagnostics13152550
24. Framme C, Schweizer P, Imesch M, Wolf S, Wolf-Schnurrbusch U (2012)Behavior of SD-OCT-detected hyperreflective foci in the retina of anti-VEGF-treated patients with diabetic macular edema.Invest Ophthalmol Vis Sci 53:5814–5818. https://doi.org/10.1167/iovs.12-9950
25. Kang JW, Chung H, Chan Kim H (2016)CORRELATION OF OPTICAL COHERENCE TOMOGRAPHIC HYPERREFLECTIVE FOCI WITH VISUAL OUTCOMES IN DIFFERENT PATTERNS OF DIABETIC MACULAR EDEMA.Retina 36:1630–1639. https://doi.org/10.1097/iae.0000000000000995
26. Yoshitake T, Murakami T, Suzuma K, Dodo Y, Fujimoto M, Tsujikawa A (2020)Hyperreflective Foci in the Outer Retinal Layers as a Predictor of the Functional Efficacy of Ranibizumab for Diabetic Macular Edema.Sci Rep 10:873. https://doi.org/10.1038/s41598-020-57646-y
27. Mo B, Zhou HY, Jiao X, Zhang F (2017)Evaluation of hyperreflective foci as a prognostic factor of visual outcome in retinal vein occlusion.Int J Ophthalmol 10:605–612. https://doi.org/10.18240/ijo.2017.04.17
28. Schneider CA, Rasband WS, Eliceiri KW (2012)NIH Image to ImageJ: 25 years of image analysis.Nat Methods 9:671–675. https://doi.org/10.1038/nmeth.2089
29. Ashrafkhorasani M, Abbasgholizadeh R, Habibi A, Emamverdi M, Nittala MG, Aghayee MM, et al (2025)Quantitative comparison of inner and outer retinal intraretinal hyperreflective foci in age-related macular degeneration.Exp Eye Res 256:110415. https://doi.org/10.1016/j.exer.2025.110415
30. Murakami T, Suzuma K, Dodo Y, Yoshitake T, Yasukura S, Nakanishi H, et al (2018)Decorrelation Signal of Diabetic Hyperreflective Foci on Optical Coherence Tomography Angiography.Sci Rep 8:8798. https://doi.org/10.1038/s41598-018-27192-9
31. Augustin S, Lam M, Lavalette S, Verschueren A, Blond F, Forster V, et al (2023)Melanophages give rise to hyperreflective foci in AMD, a disease-progression marker.J Neuroinflammation 20:28. https://doi.org/10.1186/s12974-023-02699-9

32. Bolz M, Kriechbaum K, Simader C, Deak G, Lammer J, Treu C, et al (2010)In vivo retinal morphology after grid laser treatment in diabetic macular edema.Ophthalmology 117:538–544. https://doi.org/10.1016/j.ophtha.2009.07.035
33. Mat Nor MN, Guo CX, Green CR, Squirrell D, Acosta ML (2023)Hyper-reflective dots in optical coherence tomography imaging and inflammation markers in diabetic retinopathy.J Anat 243:697–705. https://doi.org/10.1111/joa.13889
34. Mat Nor MN, Green CR, Squirrell D, Acosta ML (2025)Retinal Hyperreflective Foci Are Biomarkers of Ocular Disease: A Scoping Review With Evidence From Humans and Insights From Animal Models.J Ophthalmol 2025:9573587. https://doi.org/10.1155/joph/9573587
35. Miura M, Makita S, Sugiyama S, Hong YJ, Yasuno Y, Elsner AE, et al (2017)Evaluation of intraretinal migration of retinal pigment epithelial cells in age-related macular degeneration using polarimetric imaging.Sci Rep 7:3150. https://doi.org/10.1038/s41598-017-03529-8
36. Hammer SS, Dorweiler TF, Mcfarland D, Adu-Agyeiwaah Y, Mast N, El-Darzi N, et al (2023)Cholesterol crystal formation is a unifying pathogenic mechanism in the development of diabetic retinopathy.Diabetologia 66:1705–1718. https://doi.org/10.1007/s00125-023-05949-w
37. Vujosevic S, Bini S, Torresin T, Berton M, Midena G, Parrozzani R, et al (2017)HYPERREFLECTIVE RETINAL SPOTS IN NORMAL AND DIABETIC EYES: B-Scan and En Face Spectral Domain Optical Coherence Tomography Evaluation.Retina 37:1092–1103. https://doi.org/10.1097/iae.0000000000001304
38. Lee H, Jang H, Choi YA, Kim HC, Chung H (2018)Association Between Soluble CD14 in the Aqueous Humor and Hyperreflective Foci on Optical Coherence Tomography in Patients With Diabetic Macular Edema.Invest Ophthalmol Vis Sci 59:715–721. https://doi.org/10.1167/iovs.17-23042

Figures

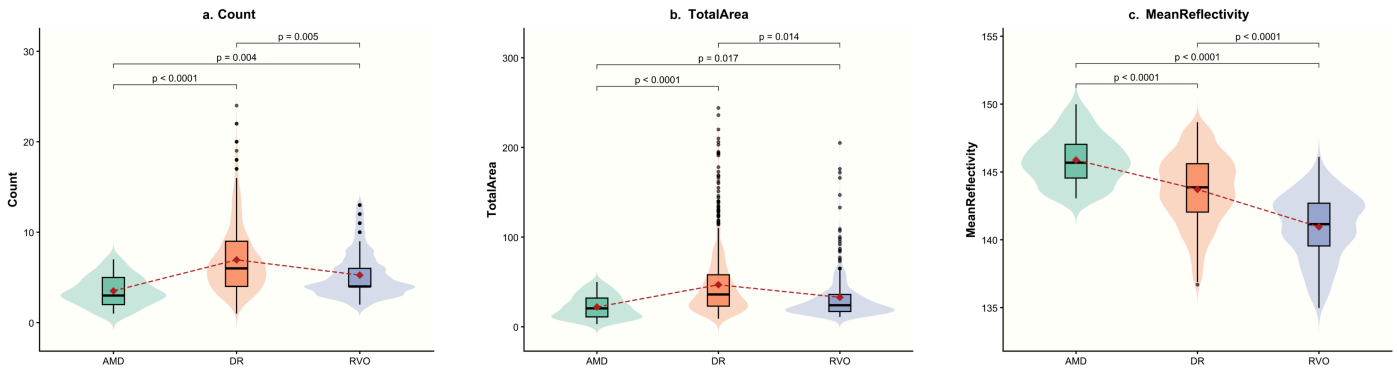


Figure 1

HRF count, total area, and mean reflectivity across AMD, DR, and RVO

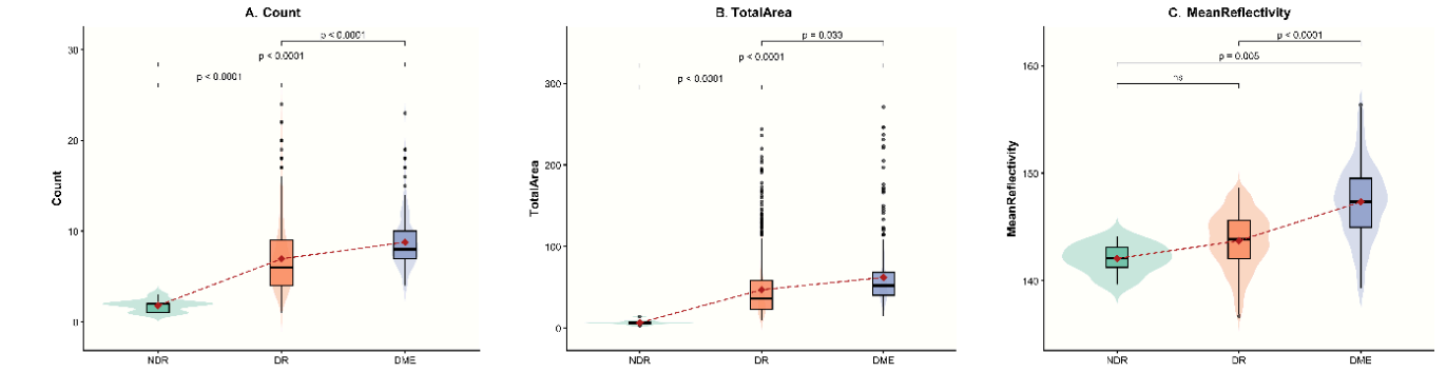


Figure 2

HRF count, total area, and mean reflectivity among NDR, DR without DME, and DME

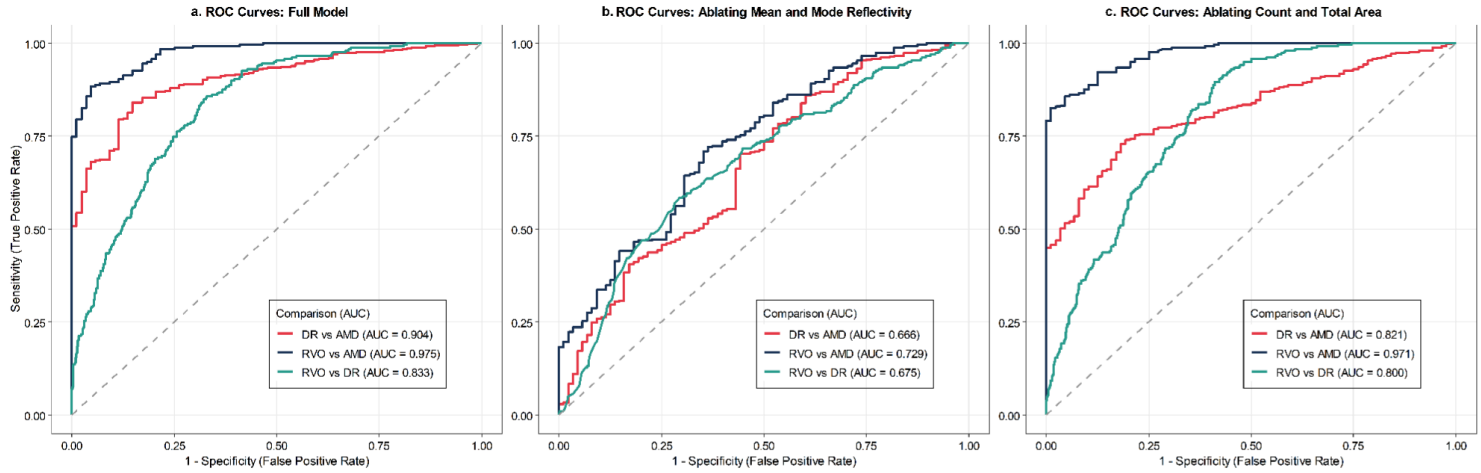


Figure 3

ROC curves for the full and ablated regression models among AMD, DR, and RVO.

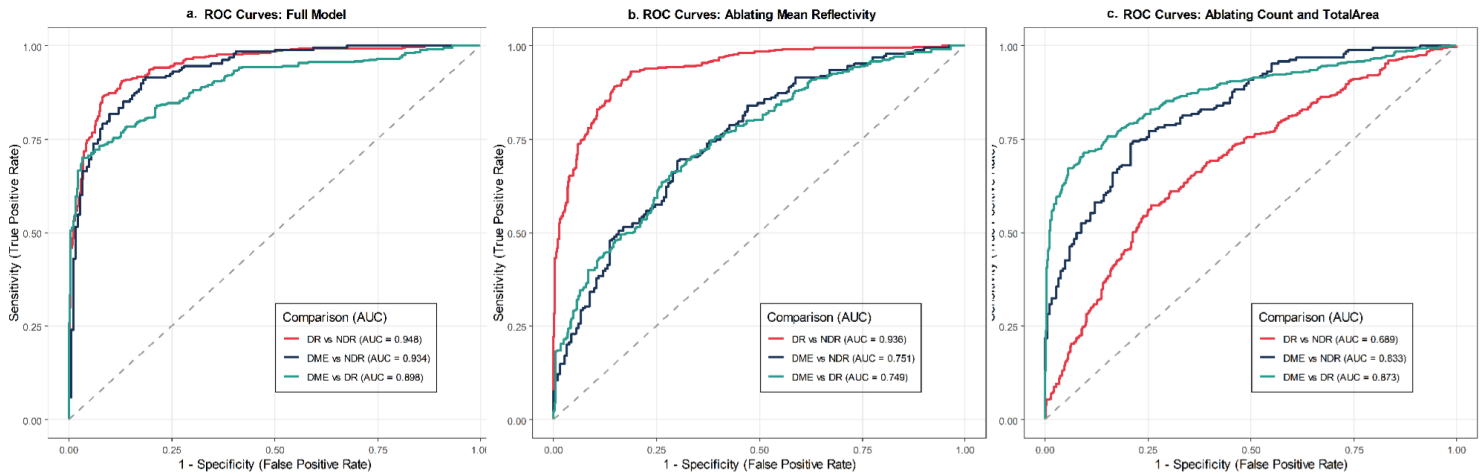


Figure 4

ROC curves for the full and ablated regression models among NDR, DR without DME, and DME.

Supplementary Files

This is a list of supplementary files associated with this preprint. Click to download.

- SupplementaryMaterials.docx